

See discussions, stats, and author profiles for this publication at: <https://www.researchgate.net/publication/228847472>

Competition between Conformational Relaxation and Intramolecular Electron Transfer within Phenothiazine–Pyrene Dyads

ARTICLE *in* THE JOURNAL OF PHYSICAL CHEMISTRY A · JUNE 2001

Impact Factor: 2.69 · DOI: 10.1021/jp0037293

CITATIONS

100

READS

36

7 AUTHORS, INCLUDING:



Jorg Daub

Universität Regensburg

198 PUBLICATIONS 4,886 CITATIONS

SEE PROFILE

Competition between Conformational Relaxation and Intramolecular Electron Transfer within Phenothiazine–Pyrene Dyads[†]

J. Daub,^{*,‡} R. Engl,[‡] J. Kurzawa,[§] S. E. Miller,^{||} S. Schneider,^{*,§} A. Stockmann,[§] and M. R. Wasielewski^{*,||}

Institut für Organische Chemie, Universität Regensburg, D-93040 Regensburg, Germany, Institut für Physikalische und Theoretische Chemie, Friedrich-Alexander-Universität Erlangen-Nürnberg, D-91058 Erlangen, Germany, and Department of Chemistry, Northwestern University, Evanston, Illinois 60208-3113

Received: October 12, 2000; In Final Form: February 1, 2001

The competition between conformational dynamics and electron transfer within a series of phenothiazine-(phenyl)_n-pyrene ($n = 0, 1$) electron donor–acceptor dyads of potential use in organic light emitting diodes was examined using femtosecond transient absorption spectroscopy. The molecular structures of these dyads permit only torsional motions around the single bonds joining each aromatic subunit. The redox properties of these molecules are nearly independent of the phenyl bridging group, whereas spectroelectrochemistry shows that the UV/vis absorption spectra of the oxidized and reduced species vary with the bridge. Each molecule exhibits dual fluorescence emission which provides evidence for conformational heterogeneity. Emission from a locally excited state originates from a minority conformation, in which electron transfer is negligible, whereas emission because of ion pair recombination results from the majority conformation which undergoes electron transfer. The electron-transfer reactions proceed with time constants <25 ps except in the dyad with the longest donor–acceptor distance in nonpolar solution, where the free energy of the charge separation reaction is positive. If electron transfer is sufficiently fast, conformational relaxation within the ion pair state product occurs on a 100–400 ps time scale, whereas if electron transfer is slow, conformation relaxation with the locally excited state centered on phenothiazine occurs. In two of the dyads in nonpolar solvents, wherein the free energy for charge separation is estimated to be very small, strong mixing between the ion pair state and the locally excited state of phenothiazine is found. The results show that competitive conformational relaxations can have a strong influence on the charge separation dynamics of donor–bridge–acceptor molecules with single bond linkages. In turn, these conformational dynamics will undoubtedly have an important influence on the photophysics of these molecules in the solid-state environment characteristic of light-emitting diodes.

1. Introduction

Molecular systems that contain several electron donors and/or acceptors tethered together using various types of bridge molecules have been extensively studied both experimentally and theoretically.^{1–15} The principal aims of these studies have been to develop a better understanding of electron transfer,^{1–6} to mimic the very efficient electron transfer in the photosynthetic reaction centers,^{2,7–9} and to develop molecular electronic devices such as optically controlled switches and gates.^{10–13} For device applications, molecular systems of the type electron donor–bridge–acceptor have been proposed as active components in organic light emitting diodes (OLEDs).^{14,15} Pilot experiments using such stilbenoid dyads with pyrene as the acceptor and phenothiazine as the donor¹⁵ have proven their potential in one-layer devices.¹⁶ To address fundamental questions regarding the influence of molecular geometry on device performance raised in an earlier work, the present study deals with pyrene/phenothiazine dyads which differ in the regiochemistry of the

covalent linkage and in the type of bridging molecule. The compounds investigated in this study are shown in Scheme 1. It was found that, depending on the nature of the bridge and its substitution pattern, the spectral distribution of the electroluminescence from these dyads can vary from being dominated by emission from locally excited (LE) states to more or less pure emission from the charge transfer (CT) state.¹⁷ At first glance, this behavior was not unexpected because in steady-state fluorescence experiments dual emission was observed. In these experiments, the relative fluorescence intensities are dependent on solvent polarity (see below). Time-resolved fluorescence measurements showed however that the rise of the CT emission is below the 30 ps time resolution of the apparatus despite the fact that at wavelengths within the LE emission band fluorescence decay times of several nanoseconds are found.¹⁸ We hypothesize that the emission properties of these dyads can be attributed to a competition between the intramolecular electron transfer dynamics and the rotational dynamics of the donor, bridge, and acceptor around the single bonds linking them. In this report, we present the results of femtosecond time-resolved transient absorption measurements which address these issues. In addition, to develop a better understanding of the excited state properties and the spectral characteristics of the photochemically created ion pairs, electrochemical and spectroelectrochemical studies are also presented.

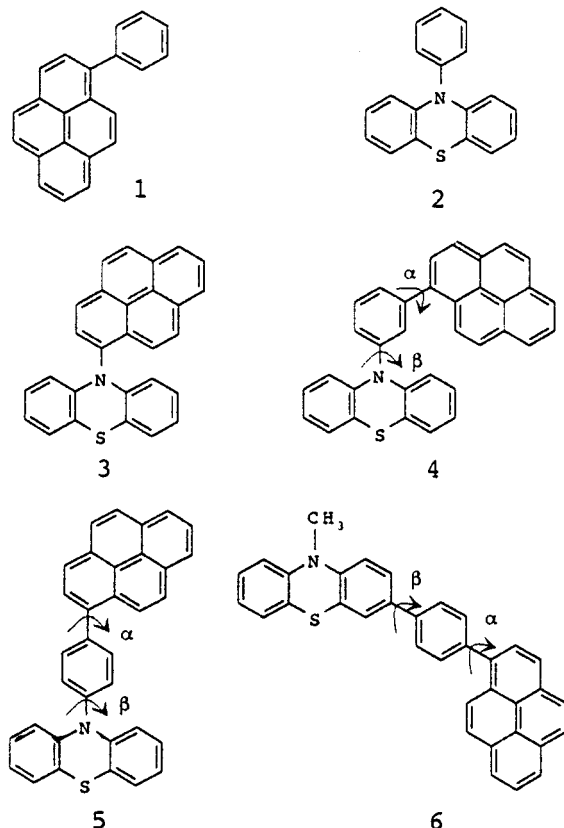
[†] Part of the special issue "Edward Schlag Festschrift".

^{*} To whom correspondence should be addressed. E-mail: schneider@chemie.uni-erlangen.de. E-mail: wasielew@chem.nwu.edu. E-mail: joerg.daub@chemie.uni-regensburg.de.

[‡] Universität Regensburg.

[§] Friedrich-Alexander-Universität Erlangen-Nürnberg.

^{||} Northwestern University.

SCHEME 1: Structures of Investigated Compounds and Abbreviations Used throughout the Text

2. Experimental Section

a. Synthesis of Compounds 1–6. A brief description of the strategies used to synthesize compounds 1–6¹⁸ is presented here. Complete details are given in the Supplementary Information. All reactions were carried out under nitrogen, and the solvents

were dried according to standard methods. The purity of the compounds was controlled by HPLC with a C₁₈ Nucleosil column.

1-Phenylpyrene (**1**)¹⁹ and 1-(4-bromophenyl)pyrene (**13**) were synthesized via the Suzuki coupling reaction²⁰ from 1-bromopyrene (**8b**) and phenylboronic acid and from 1-bromo-4-iodobenzene (**11**) and pyrenylboronic acid (**12**), respectively. 10-Phenyl-10H-phenothiazine (**2**)²¹ and 3-bromo-10-methyl-10H-phenothiazine (**9**)²² were prepared according to literature procedures. 10-(3-Bromophenyl)-10H-phenothiazine (**14**) was prepared from 1-bromo-3-iodobenzene using Ullmann coupling. The syntheses of **3–6** are shown in Scheme 2. N-Pyrenylphenothiazine (**3**) was prepared by Ullmann-type²³ coupling of phenothiazine **7** and 1-iodopyrene (**8a**; Scheme 2a). 10-[3-(Pyrene-1-yl)-phenyl]-10H-phenothiazine (**4**) is prepared using palladium catalysis as a modification of Ullmann condensation.²⁵ The key-step used in the syntheses of 3-[4-(1-pyrenyl)-phenyl]-10-methyl-10H-phenothiazine (**6**; Scheme 2b) and 10-[4-(pyrene-1-yl)-phenyl]-10H-phenothiazine (**5**; Scheme 2c) was aryl/aryl coupling using Suzuki- and Stille-type²⁴ procedures.

b. Steady-State UV/vis Absorption and Emission Spectroscopy. UV/vis absorption spectra were recorded on a Perkin-Elmer Lambda 2 spectrometer; steady-state emission spectra, on a Perkin-Elmer LS 50B. The actual values of the excitation wavelength are given in the legends to the figures.

c. Cyclic Voltammetry and Spectroelectrochemistry. For cyclic voltammetry measurements, a standard one-compartment three-electrode arrangement was used with a platinum disk as the working electrode, a platinum wire as the counter electrode, and a pseudo Ag/AgCl reference electrode. The reversible oxidation signal of ferrocenium/ferrocene (Fc⁺/Fc) was used as an internal standard. The solvent THF and the supporting electrolyte (tetrabutylammonium hexafluorophosphate TBAHFP) were purified according to standard procedures. All measurements were carried out under nitrogen and the exclusion of moisture. The cyclic voltammetry was performed with an Amel 5000 potentiostat. Spectroelectrochemistry was carried

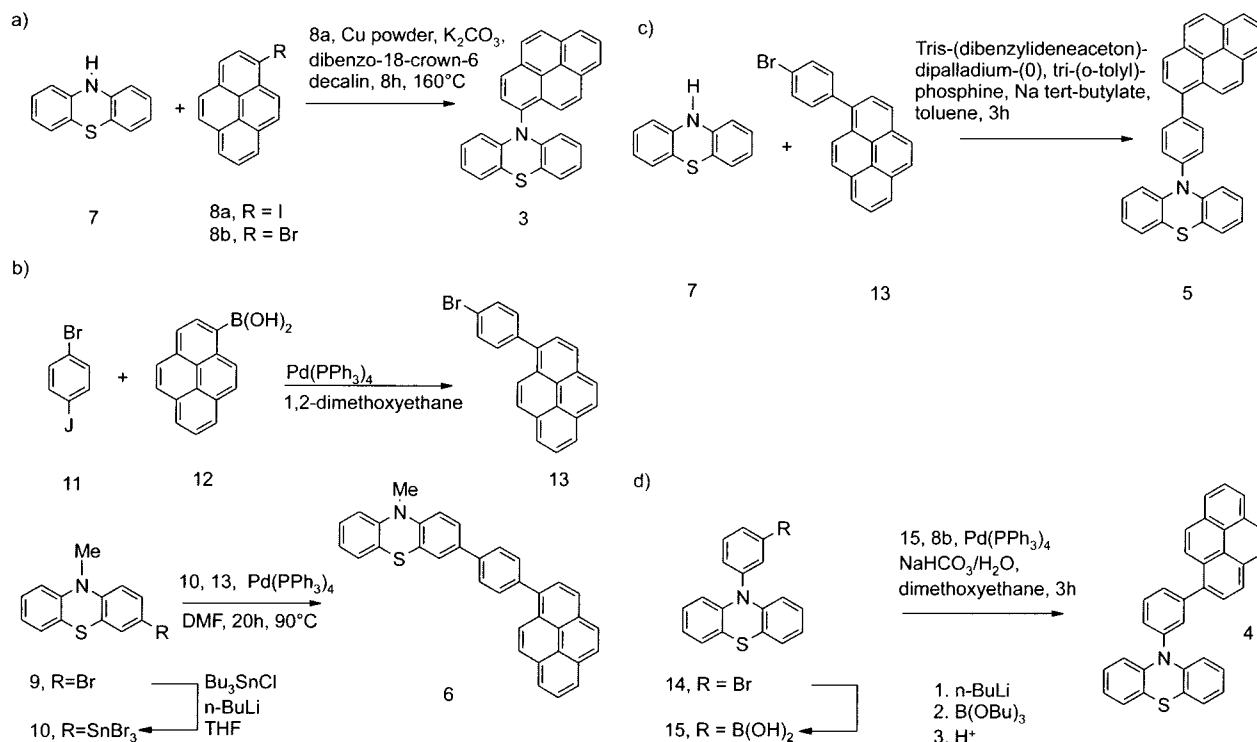
SCHEME 2: Schematic Presentation of Synthetic Route to the Investigated Compounds


TABLE 1: Selected Geometric Parameters for Compounds 1, 2, 4, and 5^a

		Distance [Å]					
compound		C7–C3/4	N1–C1	N1–C29	C29–C30	C30–S1	C33–C32
1	calcd	1.4653					
2	calcd		1.4315	1.4150	1.4162	1.6943	1.3934
4	calcd	1.4654	1.4322	1.4162	1.4160	1.6941	1.3934
	found	1.4834	1.4578	1.4183	1.4074	1.7667	1.3841
5	calcd	1.4647	1.4320	1.4159	1.4160	1.6941	1.3935
	found	1.4810	1.4384	1.4276	1.3970	1.7614	1.3675

		Torsional Angle [deg]			
compound		α	β	γ	δ
1	calcd	60.82			
2	calcd		76.56	154.70	15.40
4	calcd	54.32	78.26	155.16	15.72
	found	44.82	75.96	141.77	32.60
5	calcd	55.94	78.58	153.97	15.27
	found	51.82	80.61	146.11	28.40

^a Experimental values are compared with calculated numbers calculated using AM1. Numbering is as indicated in Figure 1 with compounds 1 and 2 numbered according to substructures of 4 and 5, respectively. Angles γ and δ are defined by the atoms C23–N1–S1–C29 and C23–C24–C30–S1.

out using an equipment described recently.²⁶ The UV/vis/NIR spectra were recorded using a Perkin-Elmer Lambda 9 spectrophotometer.

d. Transient Absorption Spectroscopy. Femtosecond transient absorption measurements were obtained using a regeneratively amplified Ti:sapphire laser described previously.⁵ Tunable femtosecond excitation pulses were generated by a two stage optical parametric amplifier (OPA).²⁷ To excite the pyrene chromophore in its 340 nm absorption band, the OPA was tuned to 680 nm and was frequency doubled using a BBO crystal. The resultant 340 nm beam was separated from the residual 680 nm light by reflection from three dichroic mirrors and was recollimated with a 100 mm f.l. lens. Typical 340 nm energies at the sample were 200–500 nJ/pulse. The polarization of the pump beam was set at the magic angle (54.7°) with respect to the probe beam to avoid anisotropic effects. The total instrument response function was 180 fs. Samples for the transient absorption experiments had optical densities at the excitation wavelength of ~0.2–0.4 (concentration $<10^{-4}$ M) in 2 mm path length cells. Samples were stirred during the experiment using a wire stirrer to prevent thermal lensing.

3. Results

a. Molecular Structure. In phenothiazine, the N–H occupies a quasiequatorial position, thus leading to conjugation between the nitrogen lone pair and the benzene rings. N-substituted phenothiazines can adopt either quasixial or quasiequatorial conformers.^{28a,b} In 10-vinylphenothiazine, both isomers (quasixial and quasiequatorial) are present as shown by photoelectron spectroscopy.²⁹ Calculations using the AM1 Hamiltonian indicate that in 10-phenylphenothiazine (2) the quasiequatorial isomer is the more stable form. X-ray structure analysis of compounds 4 and 5 leads to the structures shown in Figure 1. The phenyl group occupies the quasiequatorial position, and the structural subunits are twisted relative to each other. In Table 1, a comparison is found between experimental and calculated bond lengths for certain bonds, as well as angles α and β , which describe the degree of torsional motion about the single bond linkages, and angles γ and δ , which measure the nonplanarity of the phenothiazine moiety. In comparison with compound 2, in which the torsional angle β is small, the aryl moieties in 4 and 5 are twisted with torsional angles of almost 80°.

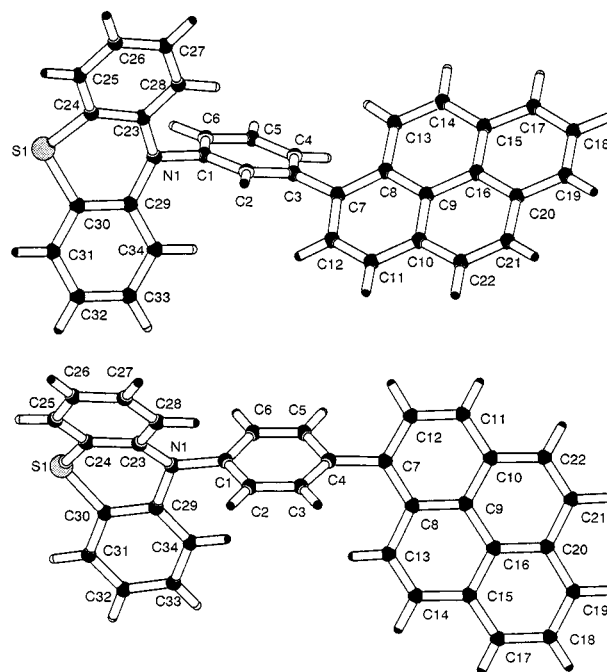


Figure 1. X-ray structure determined for compounds 4 (top) and 5 (bottom; see also Tables 1 and 2).

According to AM1 calculations, the sterically demanding pyrene group in N-pyrenylphenothiazine (3) occupies likewise the quasiequatorial position. This is also confirmed by NMR which shows H₁ and H₈ of phenothiazine shifted upfield by about 0.5 ppm. For compound 6, the AM1 calculations predict a torsional angle of $\alpha = 40^\circ$ (phenothiazine–phenyl bond) and $\beta = 56^\circ$ (phenyl–pyrene bond).

b. Steady-State UV/vis Absorption and Emission Spectra. Because we found that the UV/vis absorption spectra are fairly independent of solvent polarity, we restrict our presentation to the spectra recorded in CH₂Cl₂, Figure 2. The absorption spectrum of the phenyl-substituted pyrene, 1, around 350 nm is dominated by the longest wavelength absorption of pyrene, Figure 2a. Because the vibrational structure typical for pyrene is missing, we must conclude that there exists some interaction between the π -electronic systems of the phenyl and pyrene. According to simple AM1 calculations, the dihedral angle

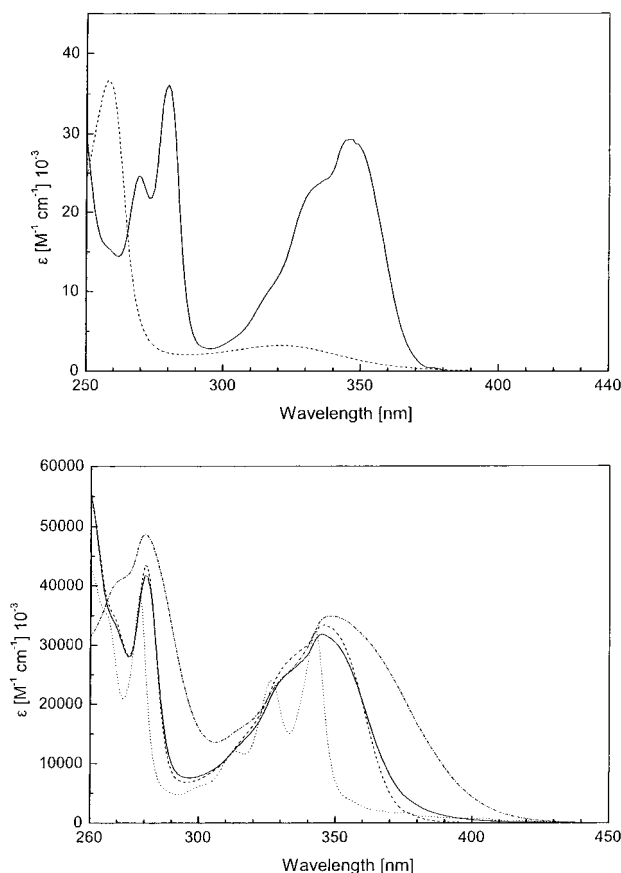


Figure 2. UV/vis absorption spectra of the compounds under investigation in CH_2Cl_2 (top) **1** (—) and **2** (---); (bottom) **3** (···), **4** (- · - ·), **5** (—), and **6** (---).

around the connecting single bond is only about 60° . The phenyl-substituted phenothiazine, **2**, exhibits a much weaker, structureless absorption because of phenothiazine in the spectral region around 350 nm, Figure 2a. In the tethered systems, **4–6**, if an excitation wavelength around 350 nm is chosen, pyrene will be preferentially excited because the extinction coefficient of pyrene is about 10 times larger than that of phenothiazine, Figure 2b.

The importance of π conjugation between pyrene and the phenyl ring is immediately obvious from a comparison of the absorption spectra of the phenyl-bridged compounds **4** and **5** with the absorption spectrum of **3**. In the latter compound, the two π -electronic systems are essentially orthogonal to each other. Because of their very small π -electronic interaction, the long wavelength absorption band of **3** corresponds essentially to that of pyrene itself. The structureless red absorption band of **4** and **5**, on the other hand, resembles that of the reference compound **1**. This finding is in accordance with the X-ray structures determined for **4** and **5** (Figure 1 and Table 1). For example, in **5**, the angle α (torsion of the single bond between pyrene and phenyl) is around 50° , whereas the angle β (torsion of the bond between phenyl and phenothiazine (N)) is about 80° . The X-ray structures also show that the phenothiazine nitrogen atom has a nonplanar geometry that resembles that of a sp^3 -hybridized, pyramidal nitrogen. Of course, one cannot exclude that the isomer found in the crystal structure is favored by packing forces rather than by intrinsic differences in free energy. If this were true, one could expect more than one isomer to be present in solution. Simple AM1 calculations predict the quasiequatorial conformer to be the most stable one. Upon systematic variation of the angle β and optimization of the

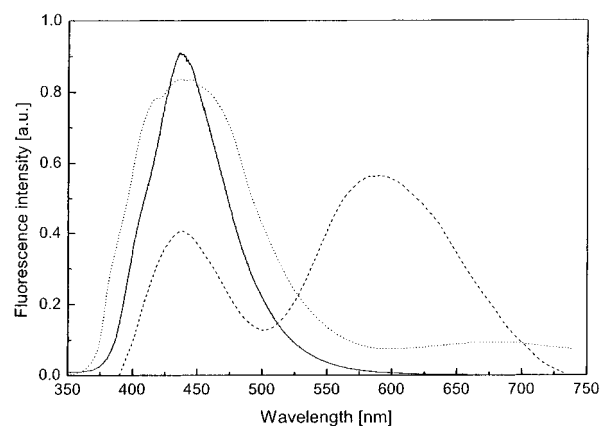


Figure 3. Fluorescence spectra of **5** in Me-CH (—), CH_2Cl_2 (---), and ACN (···); $c = 2 \times 10^{-5}$ M, $\lambda_{\text{ex}} = 300$ nm.

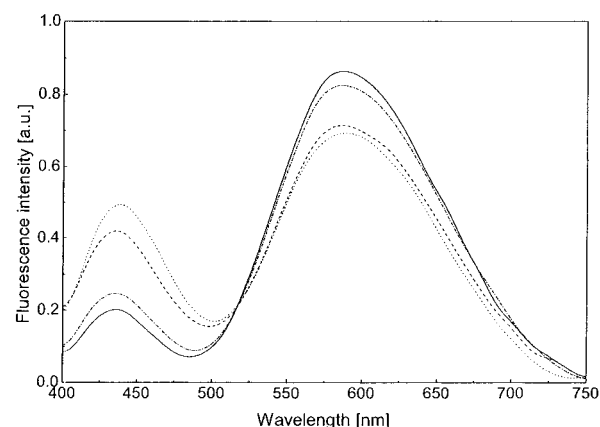


Figure 4. Variation of the fluorescence spectrum of **5** in CH_2Cl_2 with excitation wavelength, $\lambda_{\text{ex}} = 280$ (—), 287 (···), 300 (---), and 344 nm (- · - ·).

remaining structure, the heat of formation of the quasiall conformer can be estimated. In vacuo, it should be less stable by about 6 kJ/mol (J. Kurzawa, unpublished results).

The absorption spectrum of the 3-substituted phenothiazine derivative, **6**, is notably different from that of the N-substituted derivatives **4** and **5**. The most intriguing feature is the long wavelength tail extending beyond 400 nm. The hypothesis that this long-wavelength absorption is due to a CT state is contradicted by the fact that it does not change with solvent polarity. Therefore, one must conclude that its existence is due to strong π conjugation between pyrene and phenothiazine via the intermediate phenyl bridge. More sophisticated MD calculations are in progress to verify this hypothesis.

The emission spectra of **5** in methylcyclohexane, CH_2Cl_2 , and acetonitrile are compared in Figure 3. In the latter two solvents, dual emission occurs. The red emission band shows a large solvatochromic shift and can therefore unambiguously be assigned to a CT fluorescence. As has been mentioned above, the spectral distribution of the fluorescence varies with excitation wavelength, Figure 4. This fact suggests the existence of different conformers with different photophysical properties, e.g., different yields for CT formation. As one might expect, the maxima of the CT-fluorescence bands of compounds **4** and **5** are very similar and, somewhat unexpectedly, also similar to that of the directly connected system **3**.^{17,18} The CT emission of the other phenyl-bridged system, **6**, peaks at a much shorter wavelength indicating either a smaller change of the free energy of charge separation, ΔG_{CS} , or a smaller reorganization energy in the electronic ground state (see also discussion below). A

TABLE 2: Half-Wave Oxidation and Reduction Potentials of Reference Compounds and Compounds under Investigation (in THF, $c = 10^{-3}$ M, 0.1 M TBAHFP, $V = 250$ mV/s)^a

compound	oxidation: E_{ox} [V]	reduction: E_{red} [V]
<i>N</i> -methylphenothiazine ^b	0.32	
pyrene ^{30a}	0.91	−2.54
1		−2.57 ^c
2	0.33	
3	0.33	−2.47
4	0.31	−2.48
5	0.31	−2.49
6	0.31	−2.51

^a Referenced relative to Fc⁺/Fc. ^b Spreitzer, H. Ph.D. Thesis, 1995, Universität Regensburg. ^c Quasireversible wave $\Delta E = 145$ mV.

TABLE 3: Absorption Maxima of the Radical Cations and Radical Anions of Reference Compounds and Compounds 1, 2, 4, and 5 Derived from Spectroelectrochemical Experiments (cf. Figures 5–7)

compounds	formation of radical	position of absorption maxima λ_{max} [nm]
pyrene (in ACN) ^{30a}	anion	1030(w), 930(w), 735(m), 575(sh), 490(s)
<i>N</i> -methylphenothiazine (in ACN) ^a	cation	845(w), 755(w), 510(s)
1 (in THF)	anion	795, 627, 591, 539, 493
2 (in THF)	cation	866, 755, 515
4 (in THF)	cation	872, 781, 518
	anion	882, 560, 508
5 (in THF)	cation	869, 780, 515
	anion	875, 644, 563, 502

^a Spreitzer, H. Ph.D. Thesis, 1995, Universität Regensburg.

detailed description and analysis of the steady state and time-resolved emission of all investigated compounds will be given elsewhere (A. Stockmann et al., manuscript in preparation).

c. Spectroelectrochemistry and Cyclic Voltammetry. The redox potentials of compounds **1–6** as well as those of pyrene and *N*-methylphenothiazine are listed in Table 2. The oxidation potentials of *N*-methylphenothiazine and *N*-phenylphenothiazine, **2**, are almost the same. This can be explained by the fact that the phenyl substituent is in a “twisted” equatorial position, and therefore, the interaction between the phenothiazine and the phenyl subunits is negligible. All phenothiazine derivatives are reversibly oxidized at about 0.31 V. This clearly indicates that site selective oxidation occurs leading to the phenothiazine radical cation and that the intramolecular interaction in the ground states is weak. The reduction potentials of **3–6** differ only slightly and are altogether at slightly less negative potentials compared with pyrene reduction. Whereas the first reduction step in **3–6** is either reversible or quasireversible, subsequent reduction to the dianion leads to an irreversible wave which may be due to a fast protonation of the dianion. In summary, the electrochemical reduction and oxidation of the phenothiazine/pyrene dyads indicate that donor and acceptor groups behave independently and that the linker groups have almost no effect on the electrochemical properties in the ground state.

Spectroelectrochemistry confirms the findings of cyclic voltammetry that the subgroups in their ground state configuration are weakly coupled. The absorption maxima of the radical cations and radical anions of **1**, **2**, **4**, and **5** are listed in Table 3. Representative examples for radical cation and radical anion formation are shown in Figures 5–7. Because of problems with solubility of **6**, the spectroelectrochemistry of the 10-heptyl derivative **16** was investigated. The typical radical ion transitions

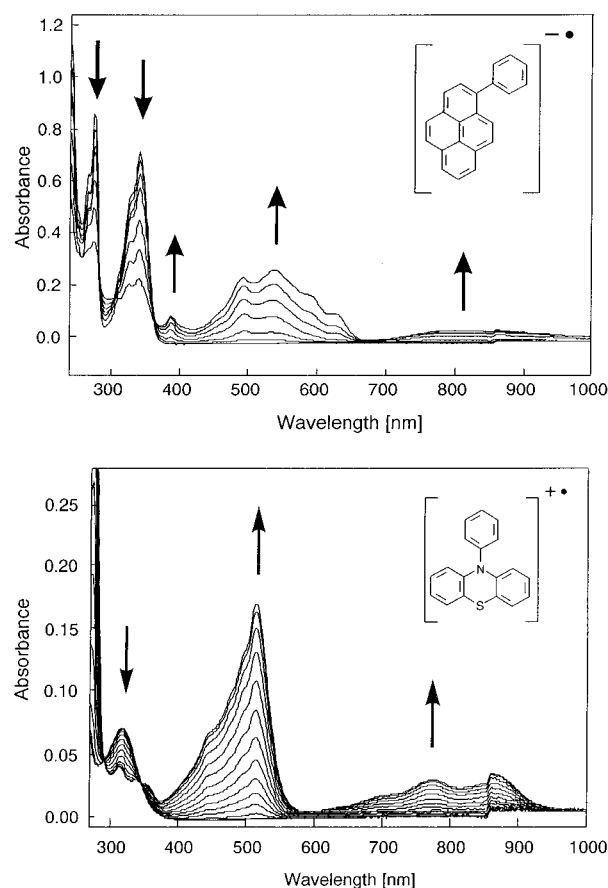


Figure 5. Evolution of the absorption spectra of the radical cations and radical anions in THF/0.1 M TBAHFP on stepwise cyclic sweep oxidation respectively reduction. (top) radical anion formation of 1-phenylpyrene **1**; (bottom) radical cation formation of 10-phenylphenothiazine **2**.

occur as a broad absorption band in the NIR region, and intense absorption bands show up between 400 and 650 nm. It is interesting to note that the spectral distribution of these red-shifted absorption bands is strongly dependent on the overall substitution pattern of the molecules. Whereas the absorption spectrum of the pyrene radical anion shows an extremely sharp peak around 490 nm,³⁰ the radical anion of phenylpyrene exhibits a rather broad band with weak vibrational structure. A similar effect is found for phenothiazine and phenylphenothiazine. It indicates a weak delocalization of the unpaired electron across the phenyl moiety. In the bridged systems **4–6**, such a delocalization is dependent on the actual linkage pattern and thus causes differences in the appearance of the absorption spectra of the reduced and oxidized species. Such a variation also shows up in the transient absorption spectra of the radical ion pairs generated by photoinduced intramolecular electron transfer (see below).

d. Transient Absorption Spectroscopy. In accordance with the well-known excited-state absorption of pyrene, we find an absorption band in the spectral region around 480–550 nm when the phenylpyrene reference compound **1** is excited at 340 nm, Figure 8. The phenylphenothiazine reference compound **2** exhibits an excited-state absorption which peaks around 650 nm. In both cases, the transient absorption rises with the instrument response time of about 200 fs. An initial fast decay with $\tau_F \approx 30$ ps is observed for both molecules. Because this decay is also observed in nonpolar solvents, it is not due to solvent reorganization. This fast relaxation may be due to a

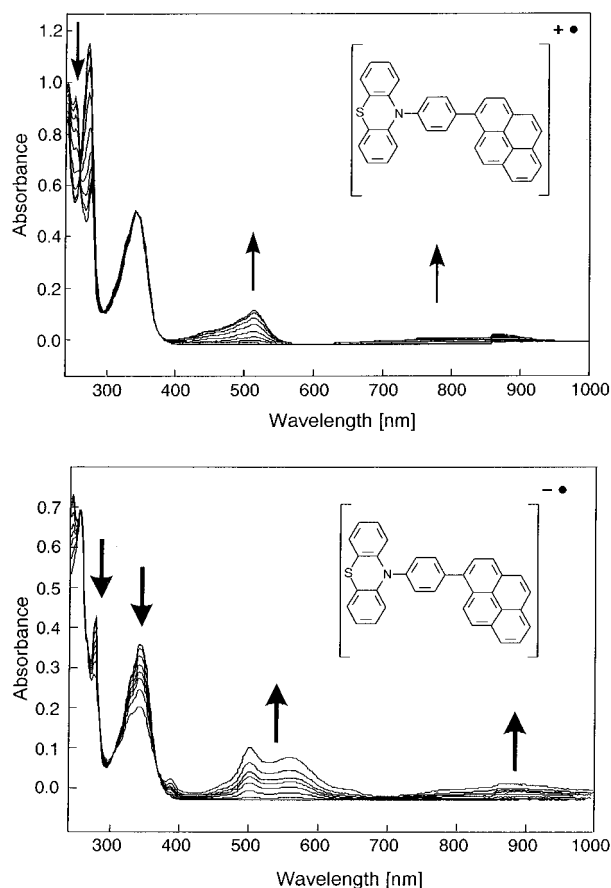


Figure 6. Formation of radical cation (top) and radical anion (bottom) of 10-[4-(1-pyrenyl)phenyl]-10-H-phenothiazine **5** in THF/0.1 M TBAHFP.

torsional relaxation around the single bond connecting the phenyl to the chromophore.

When measured with delay times of more than about 5 ps, the transient absorption spectra of the directly connected system **3** in all solvents exhibits only one fairly sharp band centered around 490 nm, Figure 9. The band decays uniformly with a decay time of several nanoseconds (cf. Table 4), which is similar to the lifetime for the CT-emission decay.¹⁸ This means that the observed transient absorption band must be due to the pyrene radical anion formed by charge separation. Additional evidence for the latter conclusion is the fact that the known absorption spectrum of the parent pyrene anion peaks at 490 nm (Table 3). The transient absorption spectra taken in Me-CH with delay times of 0.5, 3, 5, and 10 ps, respectively, demonstrate that the 490 nm absorption band of the pyrene radical anion must be nearly identical to the $S_1 \rightarrow S_n$ excited-state absorption of pyrene itself, Figure 9, because for a delay time $\Delta t = 0.5$ ps the band intensity has already reached about 75% of the maximum absorption. The fact that the maximum absorption is found for delay times around 20 ps points to a very fast electron-transfer process. Whereas the absorption around 490 nm increases upon charge separation, the absorbance above 550 nm decreases on the same time scale because in that wavelength range the excited-state absorption is larger than that of the pyrene anion.

The transient absorption spectra recorded for **5** in Me-THF and ACN are fairly similar, Figure 10a. They exhibit two major bands around 520 and 570–585 nm, respectively, with the latter one being somewhat more intense in Me-THF. In neither solvent is there much absorption at wavelengths greater than 620 nm. In Me-CH, the transient absorption appears rather broad for two reasons: (i) in the region between the two above-

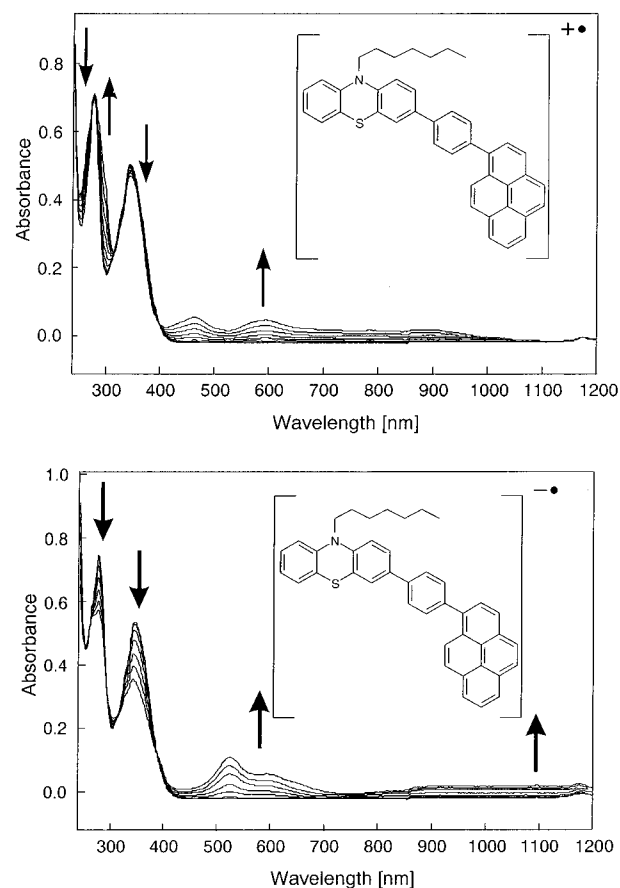


Figure 7. Formation of radical cation (top) and radical anion (bottom) of 3-[4-(1-pyrenyl)phenyl]-10-heptyl-10-H-phenothiazine **16** in THF/0.1 M TBAHFP.

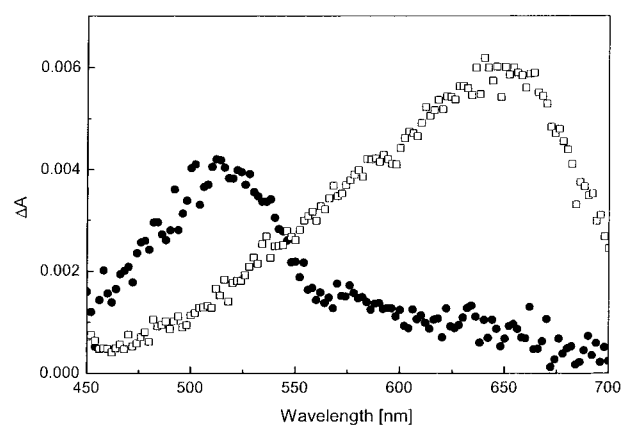


Figure 8. Transient absorption spectra of compounds **1** (●) and **2** (□) in Me-THF recorded 5 ps after excitation at 340 nm.

mentioned peaks, the absorption is also very high and (ii) one finds a fairly strong absorption around 650 nm, where the excited phenothiazine absorbs (see Figure 8). One finds that the absorption increase on the time scale of several picoseconds is not very uniform across the range 500–700 nm in contrast to the data obtained in Me-THF and ACN.

The transient kinetic behavior of the red absorption maximum is similar in all three solvents (cf. Table 4) in that the fit requires three components: a fast rising component (3.5–8 ps) of low amplitude which must be related to the electron-transfer process, a fast decaying component (80–325 ps) which could be related to a structural relaxation of the dyad geometry, and a slow component which represents the decay of the CT state. It is interesting to note that in Me-THF, a medium polarity solvent,

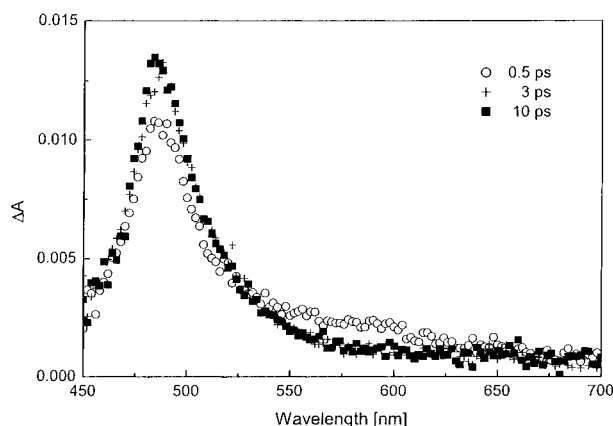


Figure 9. Transient absorption spectra of compound **3** in Me-CH recorded for different delay times: 0.5 ps (○), 3 ps (+), and 10 ps (■). Excitation wavelength was 340 nm.

TABLE 4: Rise (τ_R) and Decay Times (τ_F and τ_S) Derived from Fits of the Transient Absorption Kinetics Measured in Solvents of Different Polarity

solvent		3	4	5	6
Me-CH	τ_R [ps]	25	12	12	1.6
	τ_F [ps]			325 ^c	430 ^a
	τ_S [ps]	3000	3200	2800	3700
Me-THF	τ_R [ps]	14 ^b	6.9	5.6	5.6
	τ_F [ps]			140 ^c	400 ^c
	τ_S [ps]	3600 ^b	4600	5800	3700
ACN	τ_R [ps]	12	5.2	3.5	1.4
	τ_F [ps]			80 ^c	130 ^c
	τ_S [ps]	4000	1700	920	580

^a These components are interpreted as geometrical relaxation in the LE state. ^b Measured in CH₂Cl₂. ^c These components are interpreted as geometrical relaxation in the CT state.

5 exhibits by far the longest CT lifetime. It is possible that the CT state and the LE state of phenothiazine are in a thermal equilibrium based on the fact that in Me-CH there is a significant absorbance in the range of the phenothiazine excited-state absorption and its lifetime is reduced.

The relaxation kinetics of **5** in Me-CH at a probe wavelength of 600 nm are exactly as described before. However, at probe wavelengths in the region 450–515 nm one observes after the initial instantaneous rise a very fast decay with $\tau \approx 1.5$ ps followed by a rise with $\tau \approx 10$ ps, Figure 10b. This behavior can be explained by assuming that after excitation into the Franck–Condon state, an initial relaxation occurs leading to a state with a lower extinction coefficient for $S_1 \rightarrow S_n$ absorption or with a higher cross section for stimulated emission $S_1 \rightarrow S_0$.

If one compares the narrow transient absorption spectrum of the charge transfer state in the directly bound system **3** with the broad spectrum of the phenyl-bridged system **5**, then one can ask whether the appearance of the band around 600 nm is caused by the enlargement of the π -electron system of the pyrene anion radical or that of the phenothiazine cation radical due to conjugation with the π -electron system of the phenyl bridge. Related to this question, it is interesting to note that in derivative **4**, in which the bridge is a meta-substituted phenyl, the transient absorption spectra have a similar shape to those observed for **5** in the corresponding solvents, Figure 11. This implies also that the 600 nm peak is more intense in Me-CH and less intense in ACN than the 520 nm peak assigned to the pyrene centered radical ion. Again we find a somewhat more pronounced increase in optical density around 550 nm than around 520 nm, where the absorption rises instantaneously to a

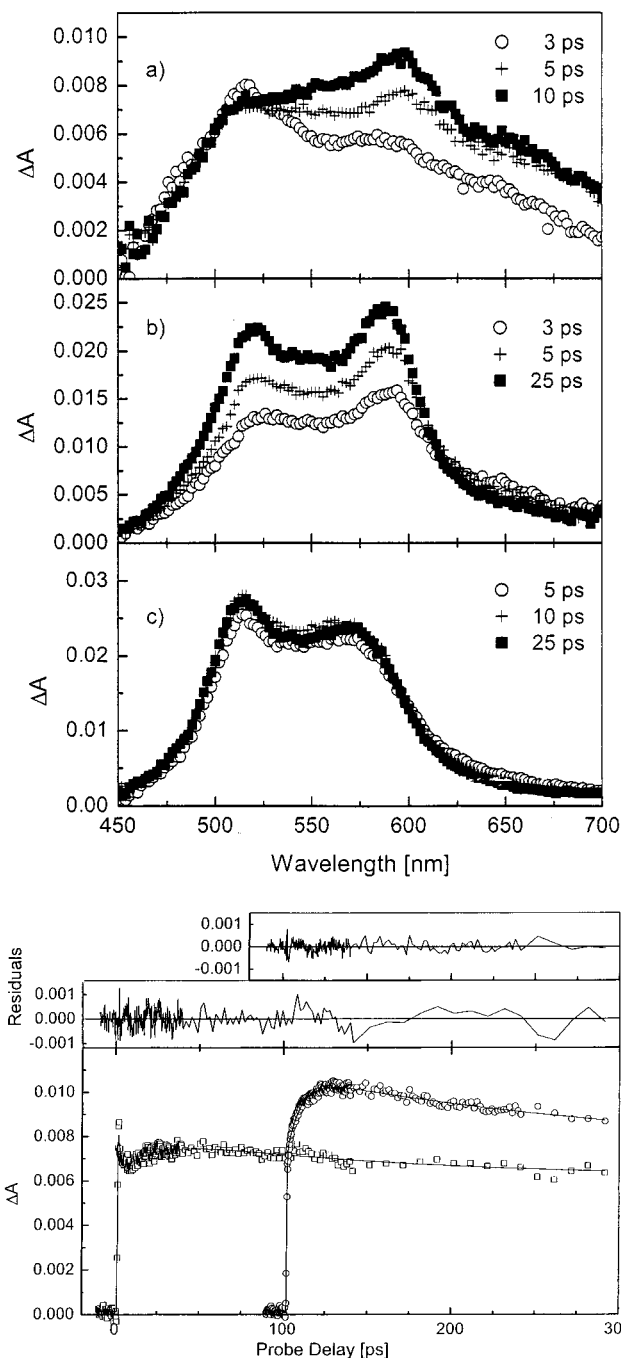


Figure 10. (top) Transient absorption spectra of compound **5** in (a) Me-CH, (b) Me-THF, and (c) ACN recorded at different delay time. Excitation wavelength was 340 nm. (bottom) Transient kinetics of compound **5** in Me-CH observed at different wavelengths: $\lambda_{det} = 515$ nm (□) and 600 nm (○, curve shifted by 100 ps). The solid lines represent fit curves.

fairly large value because of the large excited state absorption of the directly excited pyrene moiety. Therefore, the formation of the CT state is best monitored at a probe wavelength of about 575 nm.

Fitting the kinetic traces for **4** requires only one fast rising component ($\tau_R \approx 5.2$ –12 ps), a fast decaying component, and one slow decaying component (see Table 5). In view of the small amplitude found for the fast decaying component in derivative **5**, the lack of that component in the fit of the transient absorption spectra of **4** must not necessarily mean that the postulated structural relaxation does not occur. Otherwise, **4** behaves similar to **5**, in which the bridge is a para-substituted

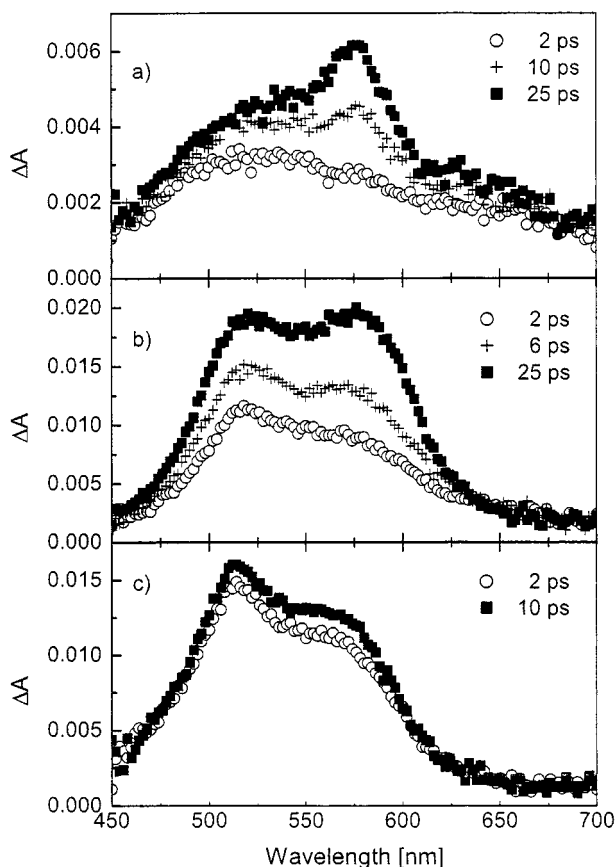


Figure 11. Transient absorption spectra of compound **4** in (a) Me-CH, (b) Me-THF, and (c) ACN recorded at different delay times. Excitation wavelength was 340 nm.

TABLE 5: Characteristic Parameters of the Systems under Investigation^a

	E_{00} [eV]	PDF [eV]	ΔG_{et} [eV] Me-CH	ΔG_{et} [eV] CH ₂ Cl ₂	ΔG_{et} [eV] ACN	R_{DA} [Å]	μ_{est} [D]
3	3.34	-0.54	-0.81	-0.98	-1.0	4.35	21
4	3.38	-0.59	-0.12	-0.87	-1.0	7.85	38
5	3.38	-0.59	-0.06	-0.85	-1.0	8.49	41
6	3.38	-0.56	0.25	-0.76	-0.98	12.8	61

^a ΔG_{et} was calculated by means of the Rehm-Weller equation.

phenyl. The lifetimes of the CT states of compounds **4** and **5** in Me-THF are also similar.

In the transient absorption spectra of derivative **6** in the nonpolar solvent Me-CH, Figure 12, we find at early times ($\Delta t = 1$ ps) a broad, structureless absorption in the wavelength region from 450 to 700 nm which can be approximated as a superposition of the excited-state absorption spectra of reference compounds **1** and **2**. The fitting of the transient kinetics shows three lifetimes: a fast rising component with about $\tau_R \approx 2$ ps, a fast decaying ($\tau_F \approx 430$ ps), and a slow component with $\tau_S \approx 4$ ns.

At first glance, the transient spectra recorded for compound **6** in Me-THF solvent are quite unusual, Figure 12. At short delay times ($\Delta t = 5$ ps), the appearance of the spectrum is dominated by the minimum around 480 nm and the maximum around 525 nm. At later times, the most striking feature is the broad minimum around 555 nm. If one keeps in mind that the emission of phenothiazene, e.g., model compound **2**, peaks around 430 nm and extends to about 500 nm, then it is obvious that the apparent reduction in transient absorbance around 480 nm at short delay times Δt is due to stimulated emission from the locally excited phenothiazene. Around 525 nm, the increase

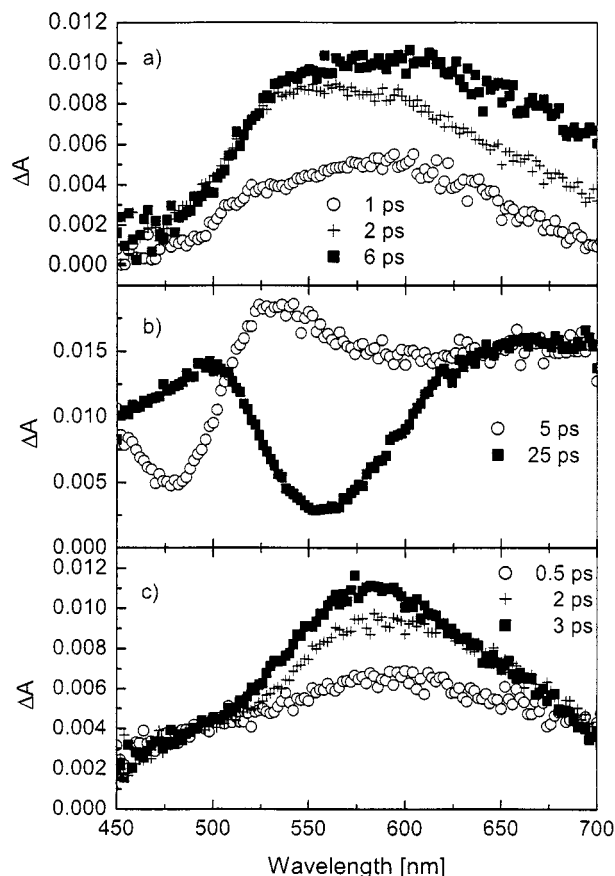


Figure 12. Transient absorption spectra of compound **6** in (a) Me-CH, (b) Me-THF, and (c) ACN recorded at different delay times. Excitation wavelength was 340 nm.

in absorbance is due to the excited state absorption of the substituted pyrene, or eventually, because of a good conjugation across the whole system, to the absorption of an excited state which is delocalized across the whole molecule (cf. also the rather broad spectrum in acetonitrile). For delay times greater than 25 ps, when charge transfer is certainly complete, the transient absorbance in the wavelength region around 550 nm is lower than expected for the absorption of the CT state because of the stimulated emission from the CT state. From the increased absorbance values between 460 and 500 nm, one can conclude that the radical ion pair (CT state) indeed exhibits a rather broad absorption band in the wavelength range 470–700 nm. The change of the signal intensity in this wavelength range is rather small once charge separation is completed because induced emission $CT \rightarrow S_0$ and radical ion pair absorption are both proportional to the number of molecules in the CT state. This expectation is nicely verified in the kinetic traces recorded at 555 nm. The formation time of the CT state is about 6 ps, whereas its decay time is around 3.7 ns. At a 680 nm probe wavelength, one also finds a fast decaying component ($\tau \approx 400$ ps), which should again reflect a structural relaxation. If the probe wavelength is 480 nm, then one observes a time course of the transient absorption which is similar to that of derivative **5** in Me-CH. After an instantaneous rise, one observes a fast decay ($\tau \approx 1.1$ ps) followed by a large increase with $\tau_R \approx 6.6$ ps. As mentioned before, the 1.1 ps decay could reflect the vibronic relaxation of locally excited pyrene.

If one switches to acetonitrile as solvent, the immediate absorbance change ($\Delta t = 0.5$ ps, cf. Figure 12) has great similarity with the superposition of the excited-state absorption spectra of the reference compounds **1** and **2**. Within an additional

picosecond, the absorption around 575 nm nearly doubles which provide evidence for a very fast transition into the CT state ($\tau_R \approx 1.4$ ps). The fast decaying component has a decay time of about 130 ps; the lifetime of the CT state is the shortest of all investigated compounds (580 ps).

The transient absorption spectra recorded from **6** in Me–CH and ACN differ greatly from those obtained for derivatives **4** and **5** in these solvents. In ACN, only one absorption maximum is found around 575 nm. In Me–CH, large absorption is observed in the wavelength range 500–600 nm, but significant absorption is also seen above 600 nm. This could again be taken as evidence that absorption from the locally excited phenothiazine contributes to the absorbance above 600 nm. In the kinetic traces, the fast decaying component can hardly be seen. This means that either structural relaxation is almost negligible or that the effect on the excited-state absorption coefficient is smaller.

4. Discussion

When dealing with photoinduced electron transfer in bridged donor–acceptor systems, the first aspect to be discussed is usually the free energy for charge separation. It can be estimated by using a simplified Rehm–Weller equation:

$$\Delta G_{\text{et}} = (E_{\text{ox}}^{\text{D}} - E_{\text{red}}^{\text{A}}) - E_{\text{oo}} + \Delta E = \text{PDF} + \Delta E \quad (1)$$

where E_{ox}^{D} and $E_{\text{red}}^{\text{A}}$ represent the oxidation and reduction potentials of donor and acceptor, and E_{oo} the excitation energy of the photoexcited species (in our case pyrene and phenylpyrene). The polar driving force, PDF, is usually determined for polar solvents such as THF (cf. Table 2). If photophysical measurements are performed in different solvents, corrections have to be made employing the relative dielectric constant of the actual solvent and effective radii for the generated radical ions. Similarly, the Coulombic energy necessary for charge separation in the actual solvent must be estimated by assuming, e.g., the separated charges to be localized at certain points within the extended donor and acceptor species. In our case, the positive charge is fixed on the nitrogen of the phenothiazine because photoelectron spectra show that the first ionization potential is N-centered, whereas the second is S-centered.^{29b} The negative charge is located in the center of pyrene. Taking into account the energy of orientational changes of the solvent molecules surrounding the reactants on basis of the Born equation, one gets

$$\Delta E = e^2/4\pi\epsilon_0[(1/2r_{\text{D}} + 1/2r_{\text{A}})(1/\epsilon_{\text{s}} - 1/\epsilon_{\text{r}}) - 1/(\epsilon_{\text{s}}R_{\text{DA}})] \quad (2)$$

where R_{DA} represents the distance between the two (localized) charges, r_{D} and r_{A} are the radii of the donor and acceptor radical ions, and ϵ_{s} and ϵ_{r} refer to the dielectric constants of the actual solvent and that in which E_{ox} and E_{red} were determined.

Because the oxidation and reduction potentials determined for the compounds studied here, Table 2, are only weakly dependent on the nature and geometry of the bridge and because the variation in the electronic excitation energy E_{oo} is also small, larger variations in ΔG_{et} are brought about only by the changes in R_{DA} . The radii of the radical ions r_{D} and r_{A} are set at a fixed value of $r = 380$ pm, which was deduced from the results of molecular modeling calculations on the AM1 level. Within the assumptions described above, the magnitude of the estimated dipole moment generated upon charge separation increases from about 20 D in **3** via about 40 D in **4** and **5** to about 60 D in the

most extended system **6**, Table 5. Therefore it is not surprising that in polar solvents (acetonitrile) photoinduced electron transfer should be exergonic by about 0.9–1.2 eV, whereas in nonpolar solvents it is strongly exergonic only in the directly coupled system **3**. Depending on the magnitude of the entropic term $T\Delta S$, which is usually neglected, and the quality of our estimated ionic radii, formation of the CT state should occur with a large rate constant in the N-linked systems **4** and **5** but probably not in **6**, which has the longest donor–acceptor distance.

In accordance with Marcus theory, the rate for charge separation can be written as

$$k_{\text{et}} = \frac{4\pi^2}{h} V^2 \text{FCWD} \quad (3)$$

with FCWD = Franck–Condon weighted density of states:

$$\text{FCWD} = (4\pi\lambda k_{\text{B}}T)^{-1/2} \exp[-(\Delta G_{\text{et}}^{\circ} + \lambda)^2/4\lambda k_{\text{B}}T] \quad (4)$$

The rate reaches a maximum when ΔG_{et} is equal to the reorganization energy λ , which is the sum of the inner (λ_{i}) and outer (λ_{o}) reorganization energy. For the phenyl-bridged systems, the outer reorganization energy can be approximated with $r = r_{\text{A}} = r_{\text{D}}$ (in Å) by³¹

$$\lambda_{\text{o}} \text{ (in eV)} = 14.43(1/r - 1/R_{\text{DA}})(1/n^2 - 1/\epsilon_{\text{s}}) \quad (5)$$

For the directly coupled system, **3**, the dipole approximation should be used because $R_{\text{DA}} \approx r_{\text{A}} \approx r_{\text{D}}$. Accordingly, the outer reorganization energy can be calculated as^{31b}

$$\lambda_{\text{o}} \text{ (in eV)} = \frac{0.624\mu_{\text{CT}}^2}{a^3} \{(\epsilon_{\text{s}} - 1)/(2\epsilon_{\text{s}} + 1) - (n^2 - 1)/(2n^2 + 1)\} \quad (6)$$

with the dipole moment μ_{CT} (in Debye) of the charge separated state and a (in Å) the radius of the solvent cavity. In nonpolar solvents, one gets $\lambda_{\text{o}} \approx 0$ eV in both cases. Therefore, the total reorganization energy in these solvents equals approximately λ_{i} . There are estimates in the literature for λ_{i} of phenothiazine derivatives, namely, $\lambda_{\text{i}} = 0.20$ – 0.27 eV³² and pyrene derivatives (formation of anion), namely, $\lambda_{\text{i}} = 0.07$ eV.³³

Using eq 6 in case of derivative **3**, one finds $\lambda_{\text{o}} = 0.33$ eV (0.47 eV) for CH_2Cl_2 (ACN). Therefore, $\Delta G_{\text{et}}^{\circ} + \lambda$ is significantly negative. Because the solvent reorganization energy increases with increasing distance R_{DA} in the phenyl-bridged systems, λ_{o} varies from 0.75 eV (1.03 eV) in derivative **4** to 1.02 eV (1.40 eV) in derivative **6** in CH_2Cl_2 (ACN) solvents. This means that the absolute magnitudes of $\Delta G_{\text{et}}^{\circ}$ and λ may actually become very close in solvents of medium and high polarity. As a consequence, photoinduced electron transfer could be faster in the phenyl-bridged systems despite the expected weaker coupling matrix element V than in derivative **3**. The data presented in Table 4 support these considerations.

As discussed earlier, phenyl substitution causes the 480 nm absorption band of the pyrene anion to spread out and extend from about 450 to 650 nm, Figure 5. It therefore overlaps strongly with the absorption of the phenyl substituted phenothiazine cation. By comparing the increase of absorbance because of radical ion formation and the decrease because of disappearance of the parent compound shown in Figures 5–7 one can estimate that the absorption by the pyrene anion is about 4 times larger than that of the phenothiazine cation. Therefore, the transient absorption induced by the generation of the radical ion pairs should be dominated by the contribution of the pyrene

anion. It is also noteworthy that changing the position of substitution on the phenothiazine causes a significant change in the absorption spectrum of the cation (compare Figures 6 and 7). These observations can qualitatively explain the shapes of the transient absorption spectra in Me-THF and ACN for which the occurrence of electron transfer is proven in all derivatives by the appearance of CT fluorescence. They also support the interpretation of electron-transfer being an important relaxation path in Me-CH for derivatives **3–5**.

From the point of view of transient absorption spectroscopy, a drawback of using pyrene as an electron acceptor is the small difference between the absorption spectra of the S_1 -excited state and of the radical anion, respectively. Evidence beyond doubt that pyrene radical anions are formed in the phenyl-bridged systems **3–5** even in nonpolar solvents could be provided by picosecond Kerr-gated Raman spectroscopy.^{34,35} These experiments also prove that in the most extended system **6** photoinduced formation of a pyrene anion does not occur in Me-CH. This raises the question of which processes are responsible for the fast rising component with small amplitude observed in the transient absorption spectra of **6** in all solvents.

Inspection of the data in Table 4 shows that the rise time assigned to charge separation in derivatives **3–5** decreases with increasing solvent polarity. This behavior is in accordance with expectation based on Marcus theory (see the discussion above). Molecule **6**, which has the longest donor–acceptor distance, shows an absorption rise in Me-CH that is faster than any rise shown by the other derivatives. This excludes the assignment of this component to photoinduced electron transfer. On the other hand, we have seen fast components ($\tau \leq 3$ ps) in the kinetic traces of this compound in Me-THF and of **5** in Me-CH which we interpreted as relaxation of the initially prepared Franck–Condon state via vibrational energy redistribution and vibrational relaxation (thermalization of the vibronic excitation). If this process causes a small increase in absorbance, it is of course difficult to detect next to the increase caused by the charge separation process. If, on the other hand, it causes directly or indirectly (e.g., via a decrease in stimulated emission) a decrease in the transient absorption, it can more readily be observed despite the following increase in absorbance because of charge separation. In the case of **6** in Me-CH, the small increase in absorbance because of vibrational relaxation can, in our opinion, be monitored because the charge separation does not occur. In favor of such an explanation is the fact that in **6** there are obviously a series of low-frequency modes which contribute to the absorption in the long wavelength tail, Figure 2.

Another feature to be explained is the occurrence of the fast decaying component ($80 \text{ ps} < \tau_F < 400 \text{ ps}$), which we assign to a conformational relaxation in the charge separated state. Conformational relaxation in electronically excited states is a well-known phenomenon. The magnitude of the torsional angle α is determined by the balance between the steric repulsion of the hydrogen atoms and the stabilization due to π -conjugation across the formal single bond. If the latter is changed upon π -electronic excitation, the equilibrium geometry (torsional angle) in the excited state differs from that of the ground state. In the case of phenothiazine, several studies^{36,37} have shown that the amount of folding around the N–S axis decreases upon formation of its radical cation (increase of the dihedral angle from about 160° to about 170°). Furthermore, photoionization studies^{29b} suggested that the amine part of phenothiazine, which is pyramidal in the neutral ground-state, adopts a more planar, sp^2 -hybridized geometry in the cationic ground state (as is well-

known for $-N^+R_2$ functional groups). It was therefore suggested that phenothiazine in its electronically excited states should undergo conformational relaxation leading toward the geometry of the radical ion. If the bending angle of the phenothiazine molecular plane changes with electronic state, then this also has an effect on the potential curve describing the rotation around the attached single bond.

The transient absorption spectra recorded for the reference compounds **1** and **2** provide direct evidence for this type of conformational relaxation to occur in solvents of low viscosity on a time scale of about 30 ps. In the phenyl-bridged systems, the relaxation process is obviously slowed and the amplitudes eventually reduced as judged by the smaller amplitudes of this component. Conformational relaxation from the Franck–Condon state should occur if no other fast relaxation process competes, like in the case of **6** in Me-CH. If, on the other hand, the circumstances are right for fast electron transfer to take place, charge separation will occur from the unrelaxed conformation and will then be followed by the conformational relaxation in the charge separated state. It is a fair assumption that the energy changes due to structural relaxation are of the same order of magnitude in both the LE and the CT state and consequently also are the observed relaxation times. Looking more closely, one finds again that the relaxation time determined for **5** increases when going from a polar to nonpolar solvent, Table 4. For **6**, such an increase is found for the pair Me-THF/ACN. In Me-CH, the relaxation time is lower than in Me-THF suggesting also that the electronic state, in which this process occurs, is different in nature, namely, LE rather than CT.

In principle, conformational relaxation should also occur in **4**. It seems that the difference in overall geometry caused by the different substitution pattern of the bridging phenyl ring must be made responsible for the difference in absolute size of the observed effect.

The compound specific dissimilarities in energy of the CT and LE states can also explain the variations in the transient absorption spectra recorded in Me-CH. Whereas in the directly coupled system **3** the CT state is lower in energy by about 0.7 eV, these two states are nearly isoenergetic in the N-substituted and phenyl-bridged systems **4** and **5**. Consequently, strong mixing of the CT state with the LE state, especially the S_1 -excited state of phenothiazine, most likely occurs. As a consequence, the absorption spectrum assigned to the CT state should show features characteristic for the phenothiazine excited-state absorption as seen in Figures 10 and 11. It appears as if this mixing is more pronounced in **5** than in **4**. This trend might reflect the electron-transfer energetics with $-\Delta G_{et}$ for **5** being smaller than that for **4**. In addition, the decay of the CT states should be enhanced because of this mixing with the LE states as is actually observed when comparing the lifetimes of **4** and **5** in Me-THF and Me-CH.

In summary, the energetic ordering of the LE states relative to the CT state as predicted from free energy estimates based on the Rehm–Weller equation allows a qualitative explanation of the results obtained by transient absorption spectroscopy. In the systems under investigation, several interesting limiting cases are realized. If electron transfer from the excited state of pyrene is highly exergonic, then charge separation occurs in less than 15 ps and is followed by conformational relaxation in the CT state. The transient absorption is characteristic for the pyrene anion. If, on the other hand, the CT state is nearly isoenergetic with the S_1 state of phenothiazine, then absorption characteristics of the $S_1 \rightarrow S_n$ absorption of phenothiazine show up in the

transient spectra. In the third case, represented by the most extended system **6** in nonpolar solvent, the CT state lies higher than the S_1 states of both the donor and the acceptor. Because electron transfer is forbidden for energetic reasons, conformational relaxation occurs in the locally excited (LE) state.

Torsion around the single bonds connecting the phenyl bridge with the donor and the acceptor is most likely the predominant internal degree of freedom responsible for the observed conformational relaxation. In addition, the bending of the molecular plane of phenothiazine could make an important contribution. Understanding the influence of these molecular motions on the photophysics of charge separation with these dyads will prove important in their application to solid state devices. It is likely that restricting conformational relaxation of the photoexcited dyads in the solid state will strongly influence the performance of these devices.

Acknowledgment. Work at Northwestern University was supported by the Division of Chemical Sciences, Office of Basic Energy Sciences, US DOE under Grant No. DE-FG02-99ER14999. Further financial support from the Volkswagenstiftung and Fonds der Chemie is also gratefully acknowledged.

Supporting Information Available: Synthesis of compounds **1–6**. This material is available free of charge via the Internet at <http://pubs.acs.org>.

Note Added after ASAP. This article was released ASAP on 4/18/2001 without a Supporting Information paragraph. The correct version was posted on 6/7/2001.

References and Notes

- (1) Paddon-Row, M. N. *Acc. Chem. Res.* **1994**, *27*, 18–25.
- (2) Wasielewski, M. R. *Chem. Rev.* **1992**, *92*, 435.
- (3) Lawson, J. M.; Paddon-Row, M. N.; Schuddeboom, W.; Warman, J. M.; Clayton, A. H. A.; Ghiggino, K. P. *J. Phys. Chem.* **1993**, *97*, 13099.
- (4) Roest, M. R.; Verhoeven, J. W.; Schuddeboom, W.; Warman, J. M.; Lawson, J. M.; Paddon-Row, M. N. *J. Am. Chem. Soc.* **1996**, *118*, 1762.
- (5) Greenfield, S. R.; Svec, W. A.; Gosztola, D.; Wasielewski, M. R. *J. Am. Chem. Soc.* **1996**, *118*, 6767–6777.
- (6) Nelson, S. F. *Chem. Eur. J.* **2000**, *6*, 581–588.
- (7) Gust, D.; Moore, T. A.; Moore, A. L. *Acc. Chem. Res.* **1993**, *26*, 198.
- (8) Kurreck, H.; Huber, M. *Angew. Chem., Int. Ed. Engl.* **1995**, *34*, 849.
- (9) Wiederrecht, G. P.; Niemczyk, M. P.; Svec, W. A.; Wasielewski, M. R. *J. Am. Chem. Soc.* **1996**, *118*, 81.
- (10) (a) Carter, F. L.; Siatkowski, R. E.; Wohltjen, H., Eds.; *Molecular Electronic Devices*; Elsevier: Amsterdam, The Netherlands, 1988. (b) Mahler, G.; May, V.; Schreiber, M., Eds.; *Molecular Electronics—Properties, Dynamics, and Applications*; Marcel Dekker: New York, 1996. (c) Jortner, J.; Ratner, M. A., Eds.; *Molecular Electronics*; Blackwell: Oxford, 1997. (d) de Silva, A. P.; Gunaratne, H. Q. N.; Gunlaugsson, T.; Huxley, A. J. M.; McCoy, C. P.; Rademacher, J. T.; Rice, T. E. *Chem. Rev.* **1997**, *97*, 1515–1566. (e) Rurack, K.; Kollmannsberger, M.; Resch-Genger, U.; Daub, J. *J. Am. Chem. Soc.* **2000**, *122*, 968–969.
- (11) Debreczeny, M. P.; Svec, W. A.; Marsh, E. M.; Wasielewski, M. R. *J. Am. Chem. Soc.* **1996**, *118*, 8174.
- (12) Debreczeny, M. P.; Svec, W. A.; Wasielewski, M. R. *Science* **1996**, *274*, 584.
- (13) (a) Gosztola, D.; Niemczyk, M. P.; Wasielewski, M. R. *J. Am. Chem. Soc.* **1998**, *120*, 5118. (b) Lukas, A. S.; Miller, S. E.; Wasielewski, M. R. *J. Phys. Chem. B* **2000**, *104*, 931.
- (14) Gong, X.; Ng, P. K.; Chan, W. K. *Adv. Mater.* **1998**, *10*, 1337–1340.
- (15) (a) Daub, J.; Beck, M.; Knorr, A.; Spreitzer, H. *Pure Appl. Chem.* **1996**, *68*, 1399–1404. (b) Knorr, A.; Daub, J. *Angew. Chem., Int. Ed. Engl.* **1995**, *34*, 2664. (c) Knorr, A.; Daub, J. *Angew. Chem., Int. Ed. Engl.* **1997**, *36*, 2817. (d) Spreitzer, H.; Scholz, J.; Gescheidt, G.; Daub, J. *Liebigs Ann.* **1996**, 2069.
- (16) (a) Kelnhofer, K.; Knorr, A.; Tak, Y.-H.; Bässler, H.; Daub, J. *Acta Polymer.* **1997**, *48*, 188. (b) Daub, J.; Kelnhofer, K.; Gareis, T.; Knorr, A.; Kollmannsberger, M.; Yoon-Heung, T.; Bässler, H. *Polymer Preprints* **1997**, *38*, 339.
- (17) Engl, R. Ph.D. Thesis, 1999, Universität Regensburg.
- (18) (a) Stockmann, A. Ph.D. Thesis, 2001, Universität Erlangen. (b) Stockmann, A.; Kurzawa, J.; Schneider, S.; Engl, R.; Daub, J. Poster presented at the VW meeting, 1999, Konstanz.
- (19) Jutz, C.; Kirchlechner, R.; Seidel, J.-H. *Chem. Ber.* **1969**, *102*, 2301–2318.
- (20) Suzuki, A. *Pure Appl. Chem.* **1994**, *66*, 213–222.
- (21) Gilman, H.; van Ess, P. R.; Shirley, D. A. *J. Am. Chem. Soc.* **1944**, *66*, 1214–1216.
- (22) Gauthier, S.; Frechet, J. M. J. *Synthesis* **1987**, 383–385.
- (23) Goshav, M.; Otroshchenko, O. S.; Sadykov, A. S. *Russ. Chem. Rev.* **1972**, *41*, 1046–1059.
- (24) Stille, J. K. *Angew. Chem.* **1986**, *98*, 504–519.
- (25) Hartwig, J. F. *Synlett* **1997**, 329–340 (Scheme 2d).
- (26) Büschel, M.; Stadler, C.; Lambert, C.; Beck, M.; Daub, J. *J. Electroanal. Chem.* **2000**, *484*, 24–32 and references therein.
- (27) Greenfield, S. R.; Wasielewski, M. R. *Opt. Lett.* **1995**, *20*, 1394–1396.
- (28) (a) Bodea, C.; Silberg, I. *Adv. Heterocycl. Chem.* **1968**, *9*, 321–460. (b) Gupta, R. R. *Phenothiazines and 1,4-Benzothiazines in Bioactive Molecules*; Elsevier: Amsterdam, The Netherlands, 1988; Vol. 4. (c) Anfinogenov, V. A.; Khlebnikov, A. I.; Filimonov, V. D.; Ogorodnikov, V. D. *Russ. J. Org. Chem.* **1970**, *35*, 458–465.
- (29) (a) Turchaninov, V. K.; Vokin, A. I.; Chipanina, N. N. *Russ. Chem. Bull.* **1998**, *47*, 1505–1513. (b) Domelsmith, N. L.; Munchhausen, L. L.; Houk, K. N. *J. Am. Chem. Soc.* **1977**, *99*, 6506–6514.
- (30) (a) Knorr, A. Ph.D. Thesis, 1995, Universität Regensburg. (b) Westermeier, C.; Gallmeier, H.-C.; Komma, M.; Daub, J. *Chem. Commun.* **1999**, 2427–2428.
- (31) (a) Hush, N. S. *Chem. Phys. Lett.* **1988**, *143*, 488. (b) Brunschwig, B. S.; Ehrenson, S.; Sutin, N. *J. Chem. Phys.* **1987**, *91*, 4714.
- (32) Borowicz, P.; Herbich, J.; Kapturkiewicz, A.; Opallo, M.; Nowacki, J. *Chem. Phys.* **1999**, *249*, 49–62.
- (33) Grampp, G.; Cebe, M.; Cebe, E. Z. *Phys. NF* **1990**, *166*, 93–101.
- (34) Schneider, S.; Kurzawa, J.; Stockmann, A.; Engl, R.; Daub, J.; Matousek, P.; Towrie, M. *Annual Report*; CLF Rutherford Appleton Laboratory: Chilton, U.K., 2000.
- (35) Zhang, S. L.; Zhu, B. F., Eds.; *International Conference on Raman Spectroscopy ICORS 2000*; J. Wiley & Sons: Chichester, U.K., 2000; p 252.
- (36) Singhabhandhu, A.; Robinson, P. D.; Fang, J. H.; Geiger, W. E., Jr. *Inorg. Chem.* **1975**, *14*, 318.
- (37) Pan, D.; Phillips, D. L. *J. Phys. Chem. A* **1999**, *103*, 4737.